

SEDust: A Pipeline for Deriving Best-Fit Spectral Energy Distributions from DUSTY Outputs

H. Mahani ^{*1} and A. Javadi¹

¹School of Astronomy, Institute for Research in Fundamental Sciences (IPM), P.O. Box 1956836613, Tehran, Iran

Abstract

In this study, we introduce **SEDust**, a pipeline designed to identify the best-fitting spectral energy distributions from the outputs of the DUSTY code and compare them to observational data. The pipeline incorporates a grid of 24000 models, enabling robust fitting for both carbon- and oxygen-rich AGB stars. It calculates key physical parameters, including luminosity, optical depth, and mass-loss rate, and produces the corresponding best-fit SED plots. Using **SEDust**, we derived the specific mass-return rates for the galaxies NGC 147 and NGC 185. The specific mass-return rate of AGB stars in NGC 147 is $8.13 \times 10^{-12} \text{ yr}^{-1}$, while in NGC 185 it is $6.52 \times 10^{-11} \text{ yr}^{-1}$. These results indicate that the mass loss from evolved stars alone cannot account for the total mass budget required to sustain these galaxies, highlighting the need for additional sources or mechanisms of mass replenishment to resolve the observed discrepancies.

Keywords: stars: evolution – stars: LPV– stars: AGB and post-AGB – stars: mass-loss – stars: carbon – galaxies: NGC 147 – galaxies: NGC 185

1. Introduction

The mass loss and dust production of evolved stars, particularly those on the asymptotic giant branch, play a key role in the dynamical evolution and chemical enrichment of galaxies by contributing material to the interstellar medium (Abdollahi et al., 2023b, Boyer et al., 2025, Javadi et al., 2011). Understanding the processes that govern dust and star formation and their dependence on stellar and environmental properties is therefore essential for insights into galactic evolution (Mahani et al., 2023). Dwarf elliptical (dE) galaxies, such as NGC 147 and NGC 185, which are satellites of Andromeda, offer valuable laboratories for studying these phenomena and are of considerable interest in modern observational astronomy because they provide important insights into the interpretation of deep redshift surveys and the evolution of stars and interstellar medium particles (Ferguson & Binggeli, 1994). While both galaxies share similarities in luminosity (Crnojević et al., 2014) and velocity dispersion (Geha et al., 2010), they exhibit notable differences.

NGC 147 contains no gas or dust and shows no evidence of recent star formation, whereas NGC 185 hosts interstellar material and shows signs of recent star formation in its central regions (De Looze et al., 2016, Marleau et al., 2010, Welch et al., 1998, Young & Lo, 1997). Photometry of the red giant branch indicates that NGC 147 has a slightly higher mean metallicity than NGC 185 (Davidge, 1994, Geha et al., 2010, McConnachie et al., 2005). Their proximity on the sky (58 arc-min) has led some to suggest they form a bound galaxy pair (van den Bergh, 1998), though kinematic studies indicate they may not be gravitationally bound (Geha et al., 2010, Watkins et al., 2013). Additionally, NGC 147 shows signs of tidal distortion, whereas NGC 185 does not (Ferguson & Mackey, 2016). Differences in star formation histories further suggest that the amounts of gas, mass loss, and dust in their interstellar media differ (Hamedani Golshan et al., 2017a,b). In this study, we aim to quantitatively test this hypothesis by estimating the mass-loss and dust injection rates in these galaxies.

^{*}mahani@ipm.ir

2. Data

To investigate the role of evolved stars in shaping the interstellar medium of NGC 147 and NGC 185, we compiled multi-wavelength datasets from several well-established catalogs. These include surveys of long-period variables, carbon-star populations, and dust-enshrouded AGBs obtained through optical, near-infrared, and mid-infrared observations. The combination of these catalogs provides a comprehensive view of the late stages of stellar evolution in both galaxies, capturing variability, chemical composition, and dust production. Such an approach enables a detailed assessment of mass-loss processes and their dependence on stellar type and environment, which is particularly relevant given the contrasting star formation histories, and interstellar medium contents of the two galaxies discussed in the introduction (Hamedani Golshan et al., 2017a, Mahani et al., 2025).

2.1. Catalogs

Long-period variables were cataloged by Lorenz et al. (2011) using i-band time-series photometry from the ALFOSC instrument on the Nordic Optical Telescope over 2.5 years with more than 30 epochs, supplemented by single-epoch K_s -band and narrow-band data. They identified 213 LPVs in NGC 147 and 513 in NGC 185, with periods between 90 and 800 days and amplitudes up to 2 mag. Near-infrared surveys of carbon stars were conducted by Sohn et al. (2006) and Kang et al. (2005) using CFHTIR, identifying 91 stars in NGC 147 and 73 in NGC 185 with J, H, K photometry. The DUSTiNGS survey (Boyer et al., 2015a,b, 2017) observed both galaxies at 3.6 and 4.5 μm across two epochs to detect variability and heavily dust-enshrouded extreme AGB stars (x-AGBs), estimating roughly 124 in NGC 147 and 99 in NGC 185. Photometric uncertainties in these datasets range from 0.02 to 0.27 mag.

Optical observations by Nowotny et al. (2001, 2003) employed V, i, TiO, and CN filters to classify O-rich (M-type) and C-rich (C-type) stars in fields of $6.5' \times 6.5'$, identifying 146 new C-stars in NGC 147 and 154 in NGC 185. Battinelli & Demers (2004a,b) further expanded the carbon-star census using the CN–TiO technique with the CFH12K camera, finding 145 C-stars in NGC 185 with a mean absolute magnitude of -4.41 ± 0.05 mag. Together, these multi-band observations provide a robust foundation for constructing spectral energy distributions and studying mass-loss rates of evolved stars in these dwarf elliptical galaxies.

2.2. SEDs

By cross-matching the available catalogs, we reconstructed the spectral energy distributions (SEDs) of LPV stars in NGC 147 and NGC 185 and incorporated their atmospheric chemistry into the modeling. The chemical classification of asymptotic giant branch (AGB) stars into oxygen-rich ($\text{C}/\text{O} < 1$) and carbon-rich ($\text{C}/\text{O} > 1$) types is a critical factor, since their atmospheric composition strongly affects the emergent SEDs (Nowotny et al., 2003). This distinction arises from the third dredge-up process, which enriches the stellar envelope with carbon, and is particularly efficient in metal-poor environments where carbon stars form more readily (Mowlavi, 1999). Properly accounting for this chemistry is therefore essential when comparing theoretical SEDs to observations.

To model these systems, we employed the radiative transfer code DUSTY (Ivezic & Elitzur, 1997), which simulates the interaction of radiation with circumstellar dust in a spherically symmetric geometry. The code solves the radiative transfer equation while incorporating absorption, scattering, and thermal re-emission, enabling realistic SEDs of dust-enshrouded stars (Abdollahi et al., 2023a, Javadi & van Loon, 2022, Javadi et al., 2013). Its flexibility in handling a wide range of dust grain properties makes it particularly suited for AGB stars with diverse dust environments. Beyond circumstellar shells, DUSTY has been widely applied to star-forming regions, interstellar dust, and active galactic nuclei, demonstrating its versatility in deriving physical parameters such as dust temperature, density distributions, and stellar mass-loss rates from observed spectra.

Given the large number of LPVs and AGB stars in our sample, manually running DUSTY through trial-and-error fitting is not feasible. To address this, we developed **SEDust**¹, an automated pipeline that employs a χ^2 minimization scheme to determine the best-fitting SEDs by comparing DUSTY model kernels with observational data. **SEDust** performs a systematic grid-based parameter exploration, incorporating variations in stellar temperature (2000–3000 K, in 100 K steps), dust temperature (500–1500 K, in 100 K steps), and optical depth (0.01–2.0, with fine increments of 0.01 below 0.5 and 0.05 above 0.5). The chemical composition

¹<https://github.com/hmahani/SEDust>

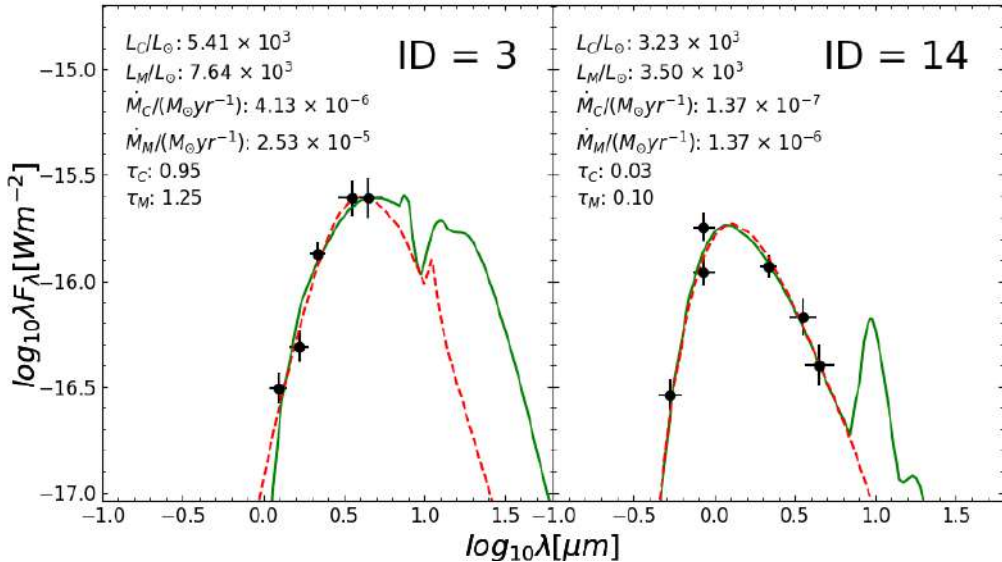


Figure 1: **SEDust** results for two example stars from the target galaxies (left: NGC 147, right: NGC 185). Stellar IDs are adopted from [Mahani et al. \(2025\)](#). The solid green curve represents the best-fit oxygen-rich model, while the red dashed curve corresponds to the best-fit carbon-rich model. Photometric uncertainties for each band are shown as error bars, based on the values reported in the original catalogs.

of the dust was tailored to the stellar type: carbon stars were modeled with a mixture of 85% amorphous carbon ([Hanner, 1988](#)) and 15% silicon carbide ([Pegourie, 1988](#)), while oxygen-rich stars were modeled with astronomical silicates ([Draine & Lee, 1984](#)). An illustration of the pipeline’s performance for different stars in both galaxies is presented in Figure 1.

SEDust was executed independently for oxygen-rich and carbon-rich AGB stars, enabling the pipeline to account for intrinsic chemical differences. The resulting grid comprised approximately 12,000 models for each stellar type, ensuring a robust coverage of parameter space. This approach allowed us to efficiently and consistently capture the diversity of SEDs across both oxygen- and carbon-rich populations, providing a reliable framework for deriving stellar and dust properties.

3. Results

Utilizing the photometric catalogs described in Section 2.1, and employing the **SEDust** pipeline outlined in Section 2.2, we derived the physical properties of AGB stars in the environments of NGC 147 and NGC 185. The use of **SEDust** allowed us to fit the SEDs of large samples of LPVs and AGB stars in a fully automated manner, ensuring consistency across the datasets. Through this method, we obtained estimates of luminosity, mass-loss rates, and dust injection rates, which serve as crucial diagnostics of the contribution of evolved stars to the interstellar medium in these two dwarf elliptical galaxies.

For NGC 147, we find that the luminosity of AGB stars spans the range from $(6.1 \pm 0.25) \times 10^2 L_\odot$ to $(7.8 \pm 0.32) \times 10^3 L_\odot$. In contrast, stars in NGC 185 show a broader luminosity distribution, extending from $(5.7 \pm 0.23) \times 10^2 L_\odot$ up to $(1.6 \pm 0.07) \times 10^4 L_\odot$. This difference suggests that NGC 185 currently hosts a larger population of bright, dust-producing AGB stars, consistent with its younger stellar population and evidence of more recent star formation compared to NGC 147 ([Hamedani Golshan et al., 2017a](#)). The derived luminosities provide not only a measure of the energy output of evolved stars but also a key input parameter for constraining their evolutionary status ([Gholami et al., 2025](#)).

In terms of mass-loss, we estimate that the contribution from LPV stars amounts to $(7.8 \pm 3.1) \times 10^{-5} M_\odot \text{ yr}^{-1}$ in NGC 147 and $(3.0 \pm 1.2) \times 10^{-4} M_\odot \text{ yr}^{-1}$ in NGC 185. When considering all AGB stars in the sample, the total mass-loss rates increase to $(9.4 \pm 3.8) \times 10^{-4} M_\odot \text{ yr}^{-1}$ for NGC 147 and $(1.6 \pm 0.6) \times 10^{-3} M_\odot \text{ yr}^{-1}$ for NGC 185. These values imply that AGB stars in NGC 185 are returning significantly more material to the interstellar medium than those in NGC 147, highlighting once again the difference in their stellar content and evolutionary histories. The corresponding dust mass injection rates are $(5.9 \pm 2.4) \times 10^{-6} M_\odot \text{ yr}^{-1}$ for NGC 147 and $(9.9 \pm 4.0) \times 10^{-6} M_\odot \text{ yr}^{-1}$ for NGC 185, further underlining

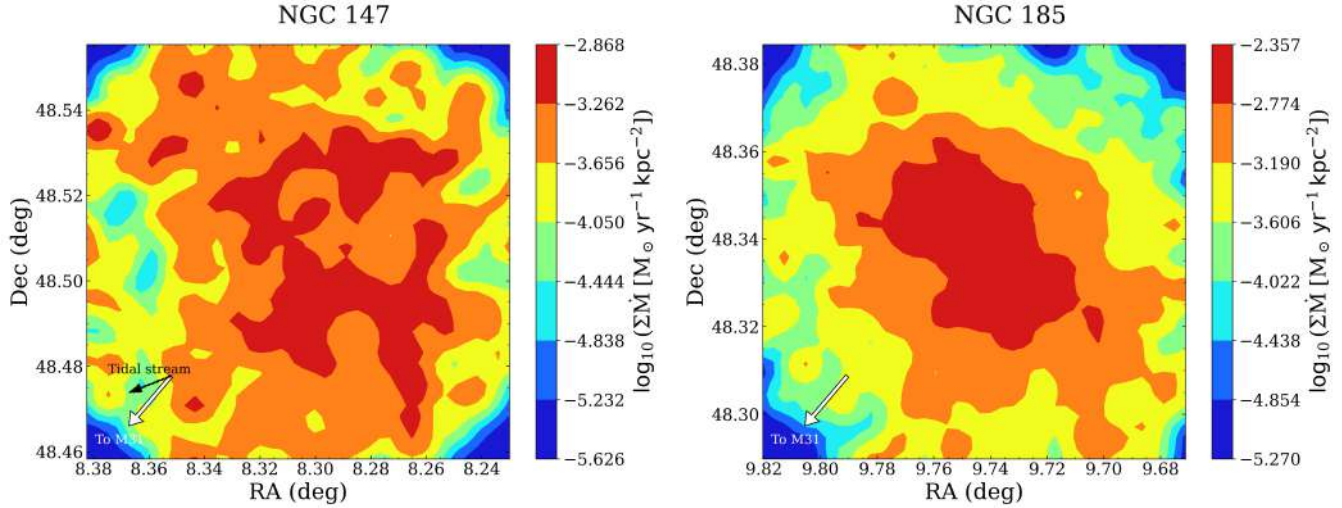


Figure 2: Surface density maps of AGB star mass-loss rates in NGC 147 and NGC 185. The white arrows mark the approximate direction toward M31, while the black arrow in the NGC 147 panel highlights the orientation of the tidal stream.

the enhanced role of NGC 185 in enriching its surrounding medium with dust.

Figure 2, a two-dimensional map of dust dispersion, indicates that gravitational interactions between NGC 147 and the Andromeda galaxy are likely influencing the distribution of dust within NGC 147. These external forces may be responsible for disturbing or stripping its interstellar material, contributing to the observed lack of recent star formation in this galaxy (Hamedani Golshan et al., 2017a). In contrast, NGC 185, which appears less affected by such interactions, retains a larger reservoir of gas and dust and continues to show signs of relatively recent star-forming activity. This environmental distinction between the two galaxies provides additional context for interpreting the measured differences in luminosity and mass-loss properties of their evolved stars.

The results of our analysis are summarized in Table 1, which presents the luminosity ranges, mass-loss rates, dust injection rates, and specific mass-return rates for both galaxies. The table also lists the replenishment timescales implied by these mass-return rates, which significantly exceed the Hubble time in both cases. This discrepancy highlights that AGB stars alone cannot supply sufficient material to sustain the stellar populations of these galaxies, and that additional sources of gas and dust (such as high-mass stars, supernovae, or external accretion) are required to explain their observed properties.

Table 1: Summary of derived properties for AGB stars in NGC 147 and NGC 185.

Parameter	NGC 147	NGC 185
Luminosity range [L_\odot]	$6.1 \times 10^2 - 7.8 \times 10^3$	$5.7 \times 10^2 - 1.6 \times 10^4$
LPV mass-loss rate [$M_\odot \text{ yr}^{-1}$]	$(7.8 \pm 3.1) \times 10^{-5}$	$(3.0 \pm 1.2) \times 10^{-4}$
Total AGB mass-loss rate [$M_\odot \text{ yr}^{-1}$]	$(9.4 \pm 3.8) \times 10^{-4}$	$(1.6 \pm 0.6) \times 10^{-3}$
Dust injection rate [$M_\odot \text{ yr}^{-1}$]	$(5.9 \pm 2.4) \times 10^{-6}$	$(9.9 \pm 4.0) \times 10^{-6}$
Specific mass-return rate [yr^{-1}]	8.13×10^{-12}	6.52×10^{-11}
Mass replenishment timescale [yr]	1.23×10^{11}	1.53×10^{10}

4. Conclusion

- We developed and applied a new automated pipeline, **SEDust**, designed to fit SEDs of AGB stars using the radiative transfer code **DUSTY**. By exploring a comprehensive parameter grid, **SEDust** enables efficient and consistent determination of key stellar properties such as luminosity, optical depth, and mass-loss rates for large stellar samples.
- The pipeline was executed separately for oxygen-rich and carbon-rich AGB stars, with more than

24000 models in total. This approach ensured that chemical composition effects were appropriately accounted for in the modeling, thereby improving the robustness of the derived physical parameters.

- Applying **SEDust** to AGB populations in NGC 147 and NGC 185, we measured luminosities, dust temperatures, and mass-loss rates. The total mass-loss rates from AGB stars were estimated to be $(9.4 \pm 3.8) \times 10^{-4} M_{\odot} \text{yr}^{-1}$ for NGC 147 and $(1.6 \pm 0.6) \times 10^{-3} M_{\odot} \text{yr}^{-1}$ for NGC 185. These translate into specific mass-return rates of $8.13 \times 10^{-12} \text{yr}^{-1}$ for NGC 147 and $6.52 \times 10^{-11} \text{yr}^{-1}$ for NGC 185.
- The inverse of these specific rates implies replenishment timescales of $1.23 \times 10^{11} \text{yr}$ for NGC 147 and $1.53 \times 10^{10} \text{yr}$ for NGC 185, both longer than the Hubble time. This demonstrates that the mass returned by evolved stars alone is insufficient to sustain the present-day stellar populations of these galaxies.
- These results highlight the necessity of additional sources of gas and dust, such as contributions from high-mass stars, supernovae, or external accretion, to explain the observed material content of dwarf galaxies. The **SEDust** pipeline thus provides a powerful and scalable tool for quantifying stellar feedback and constraining the life cycle of baryonic matter in galaxies.

References

Abdollahi H., et al., 2023a, in Wong T., Kim W.-T., eds, IAU Symposium Vol. 373, Resolving the Rise and Fall of Star Formation in Galaxies. pp 242–245, [doi:10.1017/S1743921323000339](https://doi.org/10.1017/S1743921323000339)

Abdollahi H., et al., 2023b, *Astrophys. J.*, 948, 63

Battinelli P., Demers S., 2004a, *Astron. Astrophys.*, 417, 479

Battinelli P., Demers S., 2004b, *Astron. Astrophys.*, 418, 33

Boyer M. L., et al., 2015a, *Astrophys. J. Suppl. Ser.*, 216, 10

Boyer M. L., et al., 2015b, *Astrophys. J.*, 800, 51

Boyer M. L., et al., 2017, *Astrophys. J.*, 851, 152

Boyer M. L., et al., 2025, *Astrophys. J.*, 991, 24

Crnojević D., et al., 2014, *Mon. Not. R. Astron. Soc.*, 445, 3862

Davidge T. J., 1994, *Astron. J.*, 108, 2123

De Looze I., et al., 2016, *Mon. Not. R. Astron. Soc.*, 459, 3900

Draine B. T., Lee H. M., 1984, *Astrophys. J.*, 285, 89

Ferguson H. C., Binggeli B., 1994, *Astron. Astrophys. Rev.*, 6, 67

Ferguson A. M. N., Mackey A. D., 2016, in Newberg H. J., Carlin J. L., eds, Astrophysics and Space Science Library Vol. 420, Tidal Streams in the Local Group and Beyond. p. 191 ([arXiv:1603.01993](https://arxiv.org/abs/1603.01993)), [doi:10.1007/978-3-319-19336-6_8](https://doi.org/10.1007/978-3-319-19336-6_8)

Geha M., van der Marel R. P., Guhathakurta P., Gilbert K. M., Kalirai J., Kirby E. N., 2010, *Astrophys. J.*, 711, 361

Gholami M., et al., 2025, *Astron. J.*, 170, 54

Hamedani Golshan R., Javadi A., van Loon J. T., Khosroshahi H., Saremi E., 2017a, *Mon. Not. R. Astron. Soc.*, 466, 1764

Hamedani Golshan R., Javadi A., van Loon J. T., 2017b, in Journal of Physics Conference Series. p. 012087, [doi:10.1088/1742-6596/869/1/012087](https://doi.org/10.1088/1742-6596/869/1/012087)

Hanner M., 1988, Grain optical properties., In NASA, Washington, Infrared Observations of Comets Halley and Wilson and Properties of the Grains p 22-49 (SEE N89-13330 04-89)

Ivezic Z., Elitzur M., 1997, *Mon. Not. R. Astron. Soc.*, 287, 799

Javadi A., van Loon J. T., 2022, in Decin L., Zijlstra A., Gielen C., eds, IAU Symposium Vol. 366, The Origin of Outflows in Evolved Stars. pp 210–215 ([arXiv:2204.08944](https://arxiv.org/abs/2204.08944)), [doi:10.1017/S1743921322001326](https://doi.org/10.1017/S1743921322001326)

Javadi A., van Loon J. T., Mirtorabi M. T., 2011, in Kerschbaum F., Lebzelter T., Wing R. F., eds, Astronomical Society of the Pacific Conference Series Vol. 445, Why Galaxies Care about AGB Stars II: Shining Examples and Common Inhabitants. p. 497 ([arXiv:1101.5271](https://arxiv.org/abs/1101.5271)), [doi:10.48550/arXiv.1101.5271](https://doi.org/10.48550/arXiv.1101.5271)

Javadi A., van Loon J. T., Khosroshahi H., Mirtorabi M. T., 2013, *Mon. Not. R. Astron. Soc.*, 432, 2824

Kang A., Sohn Y. J., Rhee J., Shin M., Chun M. S., Kim H.-I., 2005, *Astron. Astrophys.*, 437, 61

Lorenz D., Lebzelter T., Nowotny W., Telting J., Kerschbaum F., Olofsson H., Schwarz H. E., 2011, *Astron. Astrophys.*, **532**, A78

Mahani H., et al., 2023, in Wong T., Kim W.-T., eds, IAU Symposium Vol. 373, Resolving the Rise and Fall of Star Formation in Galaxies. pp 264–267, doi:10.1017/S1743921322004951

Mahani H., et al., 2025, arXiv e-prints, p. arXiv:2508.05596

Marleau F. R., Noriega-Crespo A., Misselt K. A., 2010, *Astrophys. J.*, **713**, 992

McConnachie A. W., Irwin M. J., Ferguson A. M. N., Ibata R. A., Lewis G. F., Tanvir N., 2005, *Mon. Not. R. Astron. Soc.*, **356**, 979

McDonald I., Zijlstra A. A., Boyer M. L., 2012, *Mon. Not. R. Astron. Soc.*, **427**, 343

Mowlavi N., 1999, *Astron. Astrophys.*, **344**, 617

Nowotny W., Kerschbaum F., Schwarz H. E., Olofsson H., 2001, *Astron. Astrophys.*, **367**, 557

Nowotny W., Kerschbaum F., Olofsson H., Schwarz H. E., 2003, *Astron. Astrophys.*, **403**, 93

Pegourie B., 1988, *Astron. Astrophys.*, **194**, 335

Sohn Y. J., Kang A., Rhee J., Shin M., Chun M. S., Kim H.-I., 2006, *Astron. Astrophys.*, **445**, 69

Watkins L. L., Evans N. W., van de Ven G., 2013, *Mon. Not. R. Astron. Soc.*, **430**, 971

Welch G. A., Sage L. J., Mitchell G. F., 1998, *Astrophys. J.*, **499**, 209

Young L. M., Lo K. Y., 1997, *Astrophys. J.*, **476**, 127

van den Bergh S., 1998, *Astron. J.*, **116**, 1688

Appendices

Appendix A Sample of Outputs

Table 2: A sample of results for NGC 147. The ID column lists the unique identifier of each star in the final catalog. Subscripts C and M correspond to the best-fit carbon and oxygen models, respectively. τ is the optical depth, L the luminosity, and \dot{M} the mass-loss rate. BC denotes the bolometric correction, and M_{ini} the initial stellar mass estimated as described in (Mahani et al., 2025). The “Chemical type” column gives the chemical classification reported in the literature, while the “Mass type” column provides the classification inferred from the initial mass.

ID	τ_C	τ_M	L_C [L_\odot]	L_M [L_\odot]	\dot{M}_C [M_\odot/yr]	\dot{M}_M [M_\odot/yr]	BC_C [mag]	BC_M [mag]	M_{ini} [M_\odot]	Chemical type	Mass type
1	0.01	0.01	3550	3400	2.07E-08	1.87E-07	3.23	3.28	1.07	C	M
2	0.2	0.41	3510	4130	1.17E-06	5.66E-06	3.17	3	1.11	C	C
3	0.95	1.25	5410	7640	4.13E-06	2.53E-05	2.52	2.14	1.01	C	M
4	0.01	0.01	6220	6420	3.03E-08	3.01E-07	3.15	3.12	1.73	C	C
5	0.02	0.02	3370	3390	3.36E-08	1.3E-07	3.25	3.24	1.18	C	C
6	0.06	0.01	3180	3170	9.65E-08	5.74E-08	3.33	3.34	1.15	C	C
7	0.85	1.15	4540	5650	2.16E-06	1.31E-05	3.05	2.81	1.31	C	C
8	0.01	0.01	4770	4940	2.58E-08	2.62E-07	3.08	3.04	1.35	C	C
9	0.02	0.01	5710	6380	5.69E-08	3E-07	3.14	3.02	1.63	C	C
10	0.01	0.01	7420	7560	3.33E-08	3.21E-07	3.09	3.07	2.01	C	C
11	0.01	0.01	4010	4200	2.51E-08	2.74E-07	3.08	3.03	1.05	C	M
12	0.01	0.01	4720	4780	2.56E-08	2.56E-07	3.19	3.18	1.34	C	C
13	0.01	0.01	1660	1800	1.48E-08	1.83E-07	2.96	2.88	0.83	C	M
14	0.02	0.01	3490	3410	3.93E-08	1.77E-07	3.21	3.23	1.1	C	C
15	0.7	0.95	4860	6520	2.67E-06	1.62E-05	2.74	2.42	1.19	C	C